Water Science & Technology

IWA PUBLISHING

Water Science & Technology Vol 84 No 3, 512 doi: 10.2166/wst.2021.226

Electrochemical degradation of chloramphenicol using Ti-based SnO_2–Sb–Ni electrode

Dan Li, Libao Zhang, Weichun Gao, Jing Meng, Yinyan Guan, Jiyan Liang* and Xinjun Shen
Shenyang University of Technology, Shenyang 110870, China
*Corresponding author. E-mail: liangjiyan2017@126.com

JL, 0000-0002-9967-8676

ABSTRACT

Antibiotic residues may be very harmful in aquatic environments, because of limited treatment efficiency of traditional treatment methods. An electrochemical system with a Ti-based SnO_2–Sb–Ni anode was developed to degrade a typical antibiotic chloramphenicol (CAP) in water. The electrode was prepared using a sol–gel method. The performance of electrode materials, impact factors and dynamic characteristics were evaluated. The Ti-based SnO_2–Sb–Ni electrode was compact and uniform as shown by characterization using SEM and XRD. The electrocatalytic oxidation of CAP was carried out in a single-chamber reactor by using a Ti-based SnO_2–Sb–Ni electrode. For 100 mg L^{-1} CAP, the CAP removal ratio of 100% and the TOC removal ratio of 60% were obtained at the current density of 20 mA cm^{-2} and in a neutral electrolyte at 300 min. Kinetic investigation has shown that the electro-oxidation of CAP on a Ti-based SnO_2–Sb–Ni electrode displayed a pseudo-first-order kinetic model. Free radical quenching experiments presented that the oxidation of CAP on Ti-based SnO_2–Sb–Ni electrode resulted from the synergistic effect of direct oxidation and indirect oxidation (·OH and $\cdot SO_4^-$). Doping Ni on the Ti/SnO_2–Sb electrode for CAP degradation was presented in this paper, showing its great application potential in the area of antibiotic and halogenated organic pollutant degradation.

Key words: chloramphenicol, electrocatalytic, Ti-based SnO_2–Sb–Ni electrode

HIGHLIGHTS

- Ti/SnO_2–Sb–Ni anodes were first applied to remove CAP by electrocatalytic oxidation.
- The removal ratios of CAP and TOC by anodic oxidation and cathodic reduction were first compared.
- The degradation of CAP on the Ti/SnO_2–Sb–Ni electrode results from the synergistic effect of direct oxidation and indirect oxidation (·OH and $\cdot SO_4^-$). $\cdot SO_4^-$ and direct oxidation contributed much to the degradation of CAP.

GRAPHICAL ABSTRACT

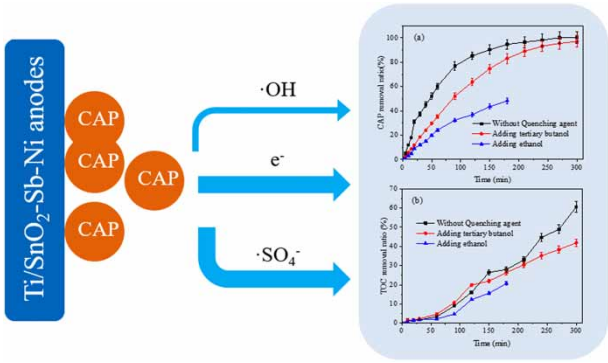

INTRODUCTION

Antibiotics have been detected in different water bodies and reported as a new environmental problem (Zhou *et al.* 2019). CAP is an effective broad-spectrum antibiotic that has been used for treating respiratory and bacterial infections in both

humans and animals (Radko *et al.* 2019; Yu *et al.* 2019). CAP is effective against several Gram-positive, Gram-negative bacteria and groups of microorganisms. It has been detected in sewage treatment plant (STP) effluents (Amildon Ricardo *et al.* 2018; Yerabham *et al.* 2020) at concentrations of 47 μg L^{-1} in China and 0.56 μg L^{-1} in Germany. Concentrations of 0.6–11.2 μg L^{-1} in China and 30–80 ng L^{-1} in Kenya (Kimosop *et al.* 2016; Yerabham *et al.* 2020) have also been reported in surface waters (SW). CAP is toxic to human health. Its presence in the aquatic environment may have harmful effects on aquatic organisms (Sun *et al.* 2019; Wu *et al.* 2020).

Most urban wastewater is treated in municipal wastewater treatment plants, but antibiotics cannot be removed to a sufficient extent (Li *et al.* 2016; Laquaz *et al.* 2020). As a consequence of the limitations of conventional wastewater treatment plants in removing antibiotics, several efforts are being made to improve the removal ratio of antibiotics, such as advanced oxidation processes (AOPs) by forming highly reactive hydroxyl radicals (·OH), especially electrochemical oxidation (EO) (Marcelino *et al.* 2015). EO process has proved to be an effective and versatile technology for the treatment of a wide range of contaminants (Hems *et al.* 2016; Moreira *et al.* 2017; Chang *et al.* 2020; Novak Jovanović *et al.* 2020). In electrooxidation, pollutants can be removed by (i) direct electrolysis, where pollutants exchange electrons directly with the anode surface without the involvement of other substances, or (ii) indirect electrolysis, where organic pollutants do not exchange electrons directly with the anode surface but rather through the mediation of some electroactive species regenerated there, which act as intermediaries for electrons shuttling between the electrode and the organic compounds (Panizza & Cerisola 2009). The (·OH) radicals with a high standard redox potential ($E_0 = 2.80$ eV) are recognized as the second-strongest oxidants after fluorine (Salazar *et al.* 2016). The ·OH radicals react rapidly and non-selective with contaminants, which are eventually mineralized into CO_2 and H_2O (Hems *et al.* 2016; Jan *et al.* 2018). These oxidizing hydroxyl radicals M(·OH) absorbed physically can be easily produced by applying a specific current to an metal oxide anode (M) surface according to the following reaction (1):

$$M + H_2O \rightarrow M(\cdot OH) + H^+ + e^- \quad (1)$$

Ti/SnO_2–Sb electrodes have been studied extensively in recent years (Stucki *et al.* 1991; Comninellis & Pulgarin 1993). To further improve the catalytic activity of the electrode, doping various metals on the surface of the electrode has become a research hotspot, such as Pt (Montilla *et al.* 2004; Berenguer *et al.* 2014; Fernández-Aguirre *et al.* 2020), Ru (Berenguer *et al.* 2014), Ni (Hamed & Amini 2011), etc. Transition metals with d-orbitals and unpaired d-electrons will form various characteristic adsorption bonds on these d-orbitals when contacting the electrons of reactant molecules to achieve the purpose of molecular activation, thus reducing the activation energy of complex reactions and promoting electrocatalytic reactions (Sharpe *et al.* 2018). Moreover, the cost of transition metals is lower than the cost of precious metals (Zhang *et al.* 2020a, 2020b).

In this work, the Ti/SnO_2–Sb electrodes doped with nickel (transition metals) were first proposed to remove CAP. A detailed investigation of reaction kinetics of CAP degradation on the Ti-based SnO_2–Sb–Ni electrode was conducted. The influence factors (applied current, initial pH, initial concentration and electrolyte) on the removal ratio and mineralization ratio were systematically investigated, and an adequate explanation was provided accordingly. The total organic carbon (TOC) and antibacterial activity were used to evaluate the entire electrochemical process.

EXPERIMENTAL

Chemicals

CAP with a purity of 98% was provided by Aladdin Industrial Corporation (Shanghai, China). Na_2SO_4, Sb_2O_3, $Ni(NO_3)_2{\cdot}6H_2O$, NaOH, NaCl, phosphoric acid, oxalate, agar powder, beef paste, peptone, glycol, ethanol, methanol and acetonitrile were provided by Da Mao Chemical Reagent Factory, China. $SnCl_4{\cdot}5H_2O$, citric acid and ammonia were provided by Dong Xing Chemical Reagent Factory, China. All chemicals were of analytical grade. Ultrapure water was obtained from a reverse osmosis control system.

Electrodes preparation

The Ti-based SnO_2–Sb–Ni electrodes were prepared using a sol–gel method. Titanium plates (purity 99.9%, 40 mm × 5 mm × 2 mm) were polished with the increasing grits (120-grit, 240-grit and 360-grit) of abrasive papers to obtain a mirror-like finish, then soaked in 40 wt% NaOH solution at 80 °C for 1 h, and then etched in 10 wt% oxalic acid for 1 h. The pre-treated titanium plates were washed with distilled water and stored in ultrapure water. The precursor solutions were prepared as follows:

the Sb_2O_3 was dissolved in concentrated HCl, the $SnCl_4{\cdot}5H_2O$ and a certain amount of $Ni(NO_3)_2{\cdot}6H_2O$ were dissolved in ethanol: the Sn:Sb:Ni molar ratio for the film preparation was 100:3:1. The total concentration of Sn ions was kept constant and was 0.5 mol L^{-1}. Citric acid and ethylene glycol were added to the metal precursor solutions. The molar ratio of metal, citric acid and ethylene glycol was 1:3:3 (Liang *et al.* 2015). The solution was stirred in a water bath (60 °C) for 60 min, and stood for 120 min to form a gel. The Ti-based SnO_2–Sb–Ni electrodes were prepared using a dip coating technique. The pretreated Ti plates were dipped in the precursor solutions for 10 min, then pulled through a liquid level at 1 mm s^{-1}. The process of dipping and raising was carried out using a coating puller machine (ZR4200, Junray, Qingdao). After that, the electrodes were dried for solvent evaporation in an infrared oven at 120 °C for 10 min, and heated in a muffle furnace under air at 450 °C for 10 min. The above procedures were repeated 15 times. Finally, the electrodes were heated in a muffle furnace at 600 °C for 2 h.

The Ti-based SnO_2–Sb electrodes were prepared in a similar method, except that nickel was not added.

Electrodes characterization

The morphologies of Ti/SnO_2–Sb–Ni electrodes were examined using a scanning electron microscopy (SEM,S8010, Hitachi, Japan). The microstructures of the electrodes were investigated by X-ray diffraction (XRD, D/max2500pc, Shimadzu, Japan), with CuKα radiation, an operating voltage of 40 kV and a current of 30 mA.

CAP electrolysis and analysis

The CAP degradation experiments were carried out in a 400 mL single-chamber reactor equipped with a magnetic stirrer at room temperature. A DC power-supply (PS-303D, Zhao Xin, China) was used for the electrolysis experiment. The self-made Ti/SnO_2–Sb–Ni electrode was used as the anode; two stainless steel substrates with the same areas were used as cathodes on both sides of the anode. The distance between the anode and the cathode was 20 mm. The experiments were carried out for a period of 300 min under different conditions. In order to explore the role of anode and cathode in the process of electrocatalytic reaction, a double chamber reactor was designed. The cathode chamber (200 mL) and anode chamber (200 mL) were separated by a cation exchange membrane. The self-made Ti/SnO_2–Sb–Ni electrode was used as the anode; the stainless steel substrate with the same areas was used as the cathode. The experiments were carried out for a period of 300 min at 20 mA cm^{-2}. During the experiment, the concentrations of CAP and TOC were measured every 30 min.

A LC1200 high-performance liquid chromatograph (Agilent), equipped with a UV-DAD detector (Agilent) and a Phenomenex C-18 column (Luna; 5 μm, 250 mm × 4.6 mm) as the stationary phase, was used to monitor the CAP concentrations during the electrolysis experiments. Phosphoric acid/acetonitrile mixtures were used as the mobile phase during the measurements. In each assay, a 10 μL sample was eluted isocratically using a 68:32 phosphoric acid/acetonitrile mixture at a flow rate of 1 mL min^{-1}. Under these conditions, the retentiontime for CAP was 14 ± 0.5 min. TOC analyser (N/C 3100, Analytik Jena AG, Germany) was used to monitor the TOC concentrations during the electrolysis experiments. The residual antibacterial activity of CAP in the degradation process was tested by *E. coli* beef extract and peptone solid medium (LB medium). Here, 3 g of beef extract, 10 g of peptone, 18 g of agar and a certain amount of sodium chloride were dissolved in 1,000 mL distilled water. The pH of the solution was adjusted to 7.0–7.2 and the solution was sterilized at 121 °C for 20 min to obtain LB medium. The LB medium was poured into a surface dish, and the Oxford cup was placed in the center of the solidified LB medium; 20 μL of sample was injected into the Oxford cup. The dish was placed in a constant temperature incubator and incubated at a specified temperature for 24 h. Finally, the diameter of bacteriostatic ring was measured.

The removal ratio of CAP (R_{CAP}) was calculated using Equation (2):

$$R_{CAP} = \frac{C_t - C_0}{C_0} \times 100\% \tag{2}$$

The removal ratio of TOC (R_{TOC}) was calculated using Equation (3):

$$R_{TOC} = \frac{\Delta(TOC)_{exp}}{C_0} \times 100\% \tag{3}$$

where, C_0 is the initial concentration of CAP (mg L^{-1}), C_t is the concentration of CAP at time t (mg L^{-1}), $\Delta(TOC)_{exp}$ is the experimental value for TOC removal at time t (mg L^{-1}).

RESULTS AND DISCUSSION

Electrode morphological characterization

The morphology of the electrodes was observed in the SEM images (Figure 1). The rough and uniformed surface of the pre-treated Ti substrate was observed in Figure 1(a). This is beneficial to form coatings(Montilla *et al.* 2004). The SEM images of Ti/SnO_2–Sb and Ti/SnO_2–Sb–Ni electrodes are shown in Figure 1(b) and 1(c). The coating particles of Ti/SnO_2–Sb electrode doped with Ni were more compact and uniform than those of the Ti/SnO_2–Sb electrode. This was beneficial for catalysis. The surface morphology of the Ti/SnO_2–Sb–Ni electrode after electrolysis of CAP was similar to that of the unused electrode, as shown in Figure 1(d). After 30 rounds of CAP degradation in the laboratory, the surface morphology of the Ti/SnO_2–Sb–Ni electrode was almost unchanged, and the effect of electrocatalytic degradation of CAP was still good.

The XRD patterns of the Ti/SnO_2–Sb, Ti/SnO_2–Sb–Ni, used Ti/SnO_2–Sb–Ni and Ti substrate are shown in Figure 2. The intensity of the diffraction peak of Ti/SnO_2–Sb electrode doped with Ni element decreases and the peak broadens slightly. This indicates that the size of crystal particles on the surface of the electrode decreased, which was conducive to the formation of active substances for electrocatalytic oxidation. No significant peaks were obtained for the nickel oxide. Ni could be embedded in SnO_2 crystal lattice in the form of atomic Ni rather than in the form of oxide crystal (Liang *et al.* 2016).

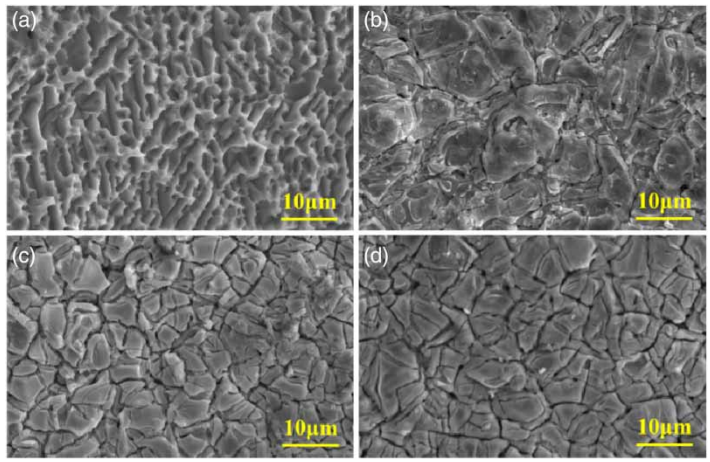

Figure 1 | The SEM images of different electrodes (a) Ti substrate, (b) Ti/SnO_2–Sb, (c) Ti/SnO_2–Sb–Ni, (d) Used Ti/SnO_2–Sb–Ni.

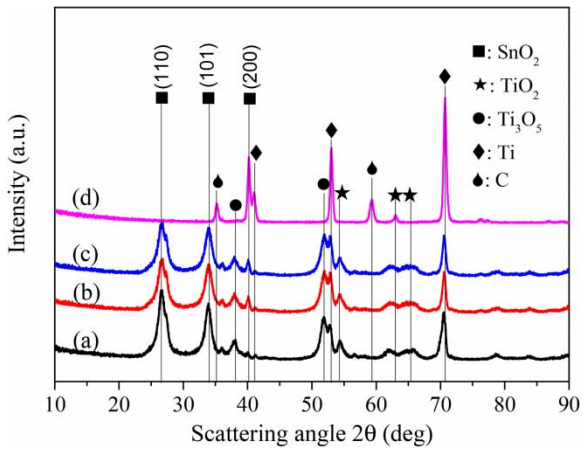

Figure 2 | The XRD patterns of different electrodes (a) Ti/SnO_2–Sb, (b) Ti/SnO_2–Sb–Ni, (c) Used Ti/SnO_2–Sb–Ni, (d) Ti substrate.

Comparison of CAP degradation on Ti/SnO_2–Sb and Ti/SnO_2–Sb–Ni electrodes

The oxidation of CAP on Ti/SnO_2–Sb and Ti/SnO_2–Sb–Ni electrodes was investigated. Each data point was the average of three independent experiments. Here, 100 mg L^{-1} CAP was electrolyzed at the current density of 20 mA cm^{-2} in a neutral solution of 35.5 g L^{-1} Na_2SO_4. The removal efficiencies of CAP and TOC on Ti/SnO_2–Sb and Ti/SnO_2–Sb–Ni electrodes were shown in Figure 3. The removal ratios of CAP on Ti/SnO_2–Sb and Ti/SnO_2–Sb–Ni electrodes were 92.50 and 100%, respectively (Figure 3(a)). The removal ratios of TOC on Ti/SnO_2–Sb and Ti/SnO_2–Sb–Ni electrodes were 45.00 and 56.78%, respectively (Figure 3(b)). The removal ratios of CAP and removal ratio of TOC on Ti/SnO_2–Sb–Ni electrode were higher than those on the Ti/SnO_2–Sb electrode. This could be because transition metal nickel has d-orbitals and unpaired d-electrons. When it contacts the electron of reactants, various characteristic adsorption bonds are formed on the d-orbitals (Sharpe *et al.* 2018). This is beneficial to the oxidation of CAP and by-products. Moreover, the surface morphology of the electrode has a certain effect, as shown by SEM. The influence of the production of active substances on CAP oxidation is discussed in the following sections. Therefore, the Ti/SnO_2–Sb–Ni electrode had a better performance for CAP oxidation than the Ti/SnO_2–Sb electrode. Additionally, the electrodes can be reused more than 30 times with good stability.

Impact factor analysis

In this part, the effects of current density, initial pH, initial CAP concentration and electrolyte on CAP removal by using Ti/SnO_2–Sb–Ni as anode are discussed. Each data point was the average of three independent experiments.

Effect of current density

The effect of applied current density ($i = 10$–30 mA cm^{-2}) on EO process parameters by Ti/SnO_2–Sb–Ni electrodes was studied systematically under the conditions of pH 7, the initial concentration of CAP 100 mg L^{-1}($C_0 = 100$ mg L^{-1}), and the initial concentration of Na_2SO_4 35.5 g L^{-1}($S_0 = 35.5$ g L^{-1}). Figure 4(a) shows the effect of different values of applied i (mA cm^{-2}) on the electrolytic removal ratio of CAP. When i value increased from 10 to 20 mA cm^{-2}, the removal ratio of CAP increased from 39.98% to 100%. With the increase of applied current, the number of oxidant species (chemisorbed and physiosorbed ·OH) produced on the surface of the anode increased significantly, which improved the removal ratio of CAP (Rubí-Juárez *et al.* 2016; Kaur *et al.* 2018). When i value increased from 20 to 30 mA cm^{-2}, the removal ratio decreased from 100% to 81.19%. The inevitable reaction of oxygen evolution on an anode surface at high current intensity competed with the removal of CAP, which resulted in the decrease of the removal ratio of CAP (He *et al.* 2019; Kaur *et al.* 2019). The removal ratio of CAP at 300 min was the highest, approaching 100%, at the applied current density of 20 mA cm^{-2}.

TOC removal ratio was tested in the same range of current density (10–30 mA cm^{-2}) (Figure 4(b)). When the current density was 20 mA cm^{-2}, the removal ratio of TOC was the highest and reached 56.78%, indicating that most of the organic matter was converted into inorganic matter, and the mineralization ratio was better without secondary pollution.

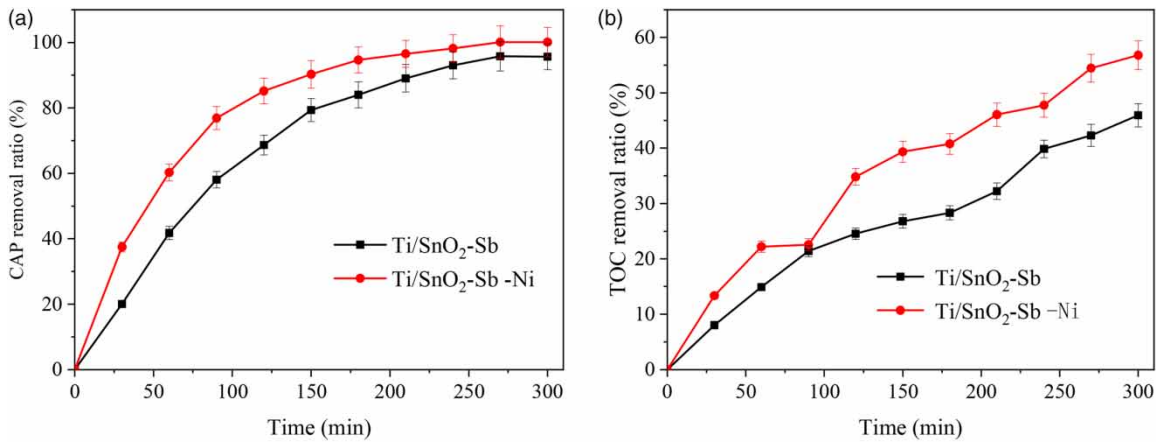

Figure 3 | (a) CAP removal ratio and (b) TOC removal ratio on Ti/SnO_2–Sb and Ti/SnO_2–Sb–Ni electrodes.

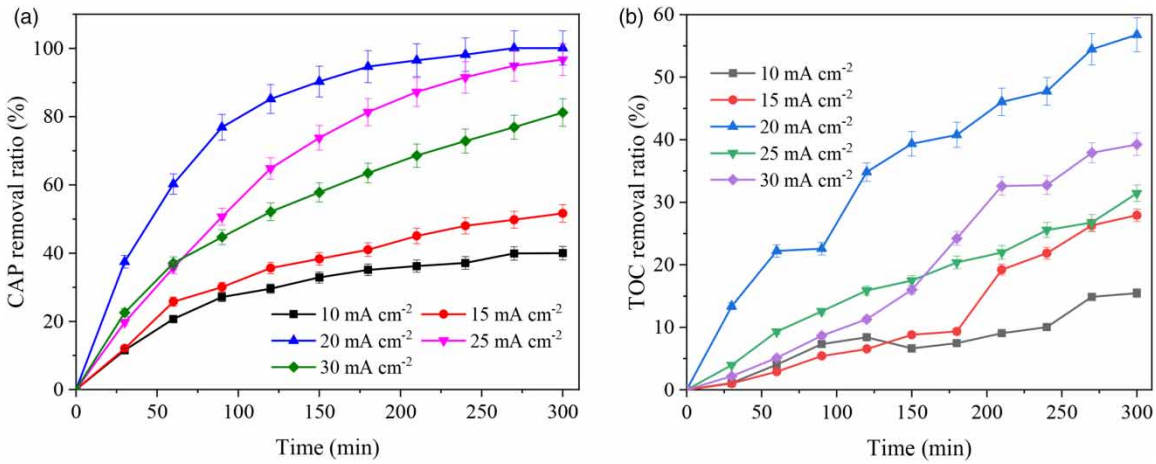

Figure 4 | Effect of applied current density on (a) CAP removal ratio and (b) TOC removal ratio.

Effect of initial pH

The removal ratio of organic pollutants by EO is highly correlated with the pH value. The property of various oxidation species generated on the anode surface and in the bulk solution largely depends on the pH of the treated wastewater. Effect of initial pH (3–11) of the solution on CAP removal ratio (Figure 5(a)) and TOC removal ratio (Figure 5(b)) was studied at $i = 20$ mA cm^{-2}, $C_0 = 100$ mg L^{-1} and $S_0 = 35.5$ g L^{-1}. As shown in Figure 4(a), the removal ratio of CAP increased with time. With the increase of solution pH from 3 to 7, the removal ratio of CAP first decreased and then increased. CAP removal ratio weakened with the increase of the solution pH from 7 to 11. CAP removal ratio is the highest at pH 3 and 7, close to 100%. This is because the anodic oxygen evolution potential in acidic solution is high and competitive oxygen evolution reaction does not easily occur. With the increase of pH value, the oxidation potential of ·OH decreases and the oxidation ability decreases, which results in the decrease of CAP degradation ratio. When pH continues to rise to 7, H^+ in the solution is neutralized, which is conducive to the formation of ·OH. When the pH value reaches 11, the solution is in a strong alkali state, and the oxygen evolution potential decreases, which is prone to oxygen evolution reaction (Qiang *et al.* 2010; Asim *et al.* 2017). As shown in Figure 4(b), TOC removal ratio was 60.60% and 56.68% at pH 3 and 7, respectively. This indicated that most of the organic matter was degraded into inorganic matter without secondary pollution. Therefore, for the neutral CAP wastewater, it was not necessary to adjust the initial pH to effectively remove CAP by electrocatalytic oxidation.

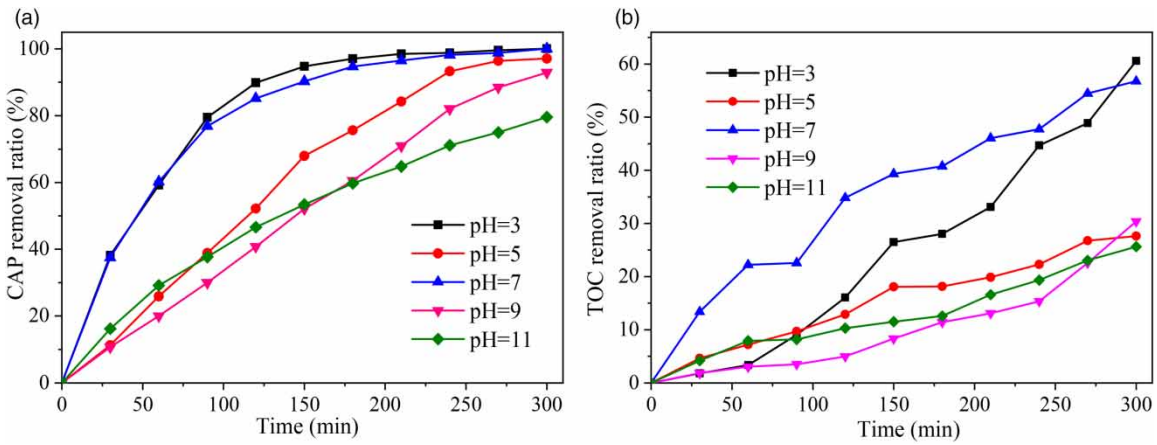

Figure 5 | Effect of initial pH on (a) CAP removal ratio and (b) TOC removal ratio.

Effect of initial CAP concentration and kinetics

The effect of initial CAP concentration (50–200 mg L^{-1}) of the solution on CAP removal ratio (Figure 6(a)) and TOC removal ratio (Figure 6(b)) was studied at i = 20 mA cm^{-2}, pH = 7 and S_0 = 35.5 g L^{-1}. It is shown in the figure that the degradation ratio of CAP was as high as 90% with the initial concentration of CAP from 50 to 200 mg L^{-1} and the electrolysis time was 300 min. Compared with other concentrations, the degradation ratio of CAP at an initial concentration of 200 mg L^{-1} at 300 min was apparently lower. This may due to the degradation ratio of CAP, which decreases slightly as the concentration of CAP increases, and the intermediate product consumes part of ·OH to compete with CAP. Conversely, the concentration of CAP was too high to degrade CAP completely in the system. It is shown in the figure that the removal ratio of TOC by electrocatalytic oxidation of CAP with medium concentration (80 mg L^{-1} and 100 mg L^{-1}) was approximately 60.0%.

The CAP removal by electrocatalytic oxidation on the Ni^{2+}-doped Ti/SnO_2–Sb electrode with time can be represented by a pseudo-first-order model which was given as:

$$-\frac{dC}{dt} = kC \tag{4}$$

$$\ln\frac{C_0}{C_t} = kt \tag{5}$$

where, C is the CAP concentration (mg L^{-1}), k is CAP removal constant (min^{-1}), and t is reaction time (min).

Kinetics curve parameters of CAP removal on Ni^{2+}-doped Ti/SnO_2–Sb electrode at different initial CAP concentrations are shown in Figure 7. In the figure, ln(C_0/C_t) was linear with time. The correlation coefficients were 0.982, 0.981, 0.997, 0.996 and 0.998 at different initial CAP concentrations (50 mg L^{-1}, 80 mg L^{-1}, 100 mg L^{-1}, 150 mg L^{-1} and 200 mg L^{-1}), respectively. This indicated that the oxidation of CAP on the Ni^{2+}-doped Ti/SnO_2–Sb electrode displayed pseudo-first-order kinetic behavior. The higher the initial concentration of CAP, the higher was the reaction rate constant and the higher was the reaction rate.

Effect of electrolyte

Figure 8 shows the time-dependent curves of CAP and TOC removal ratio in different electrolyte types (Na_2SO_4, $NaNO_3$ and NaCl) under the conditions of i = 20 mA cm^{-2}, S_0 = 35.5 g L^{-1}, C_0 = 100 mg L^{-1}. NO_3^- is stable in water. In the electrolysis system, NO_3^- cannot react with CAP, and cannot compete with CAP for free radicals. The addition of NO_3^- only improved the conductivity of the solution and promoted electron transfer. When the electrolyte was $NaNO_3$, the removal ratio of CAP was lower than that of the other two electrolytes. In the solution of Na_2SO_4 and NaCl, the removal ratio of CAP was close to 100.0%. The TOC removal ratio (56.68%) in the solution of $NaSO_4$ was higher than that in other solutions. Chloride ion can quench ·OH to produce some radicals with weak oxidation ability ($HOCl^-$·, etc.) (Equation (9)). Therefore, the removal ratio of TOC in NaCl solution was low. In an electrocatalytic oxidation system, some SO_4^- in solution may be activated

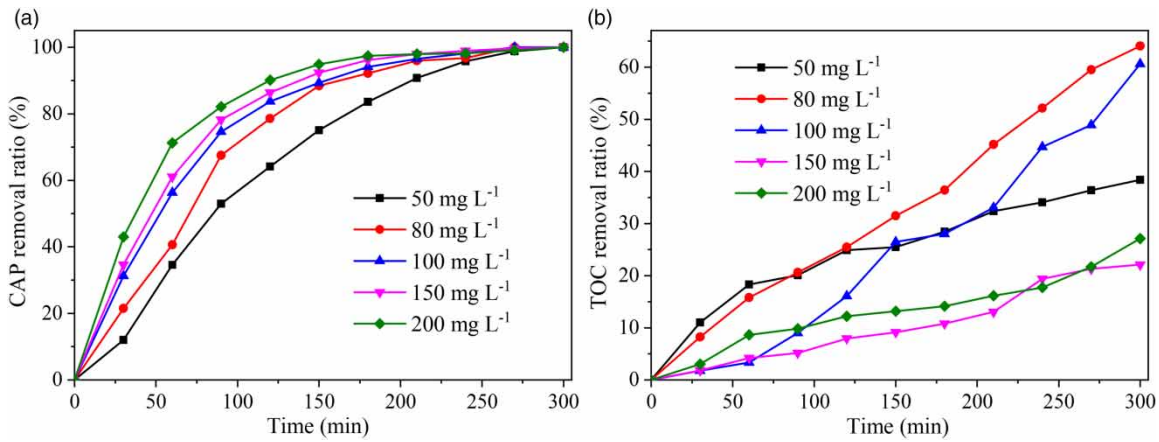

Figure 6 | Effect of initial CAP concentration on (a) CAP removal ratio and (b) TOC removal ratio.

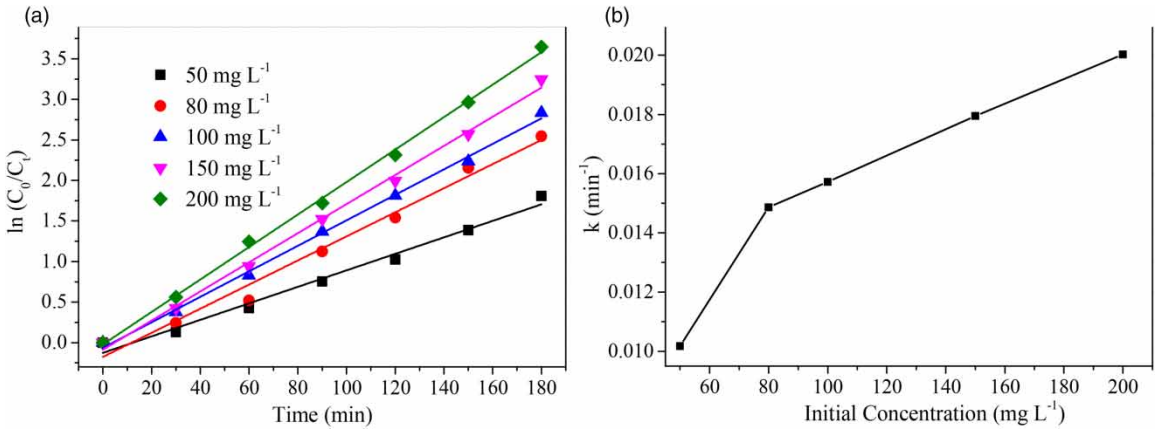

Figure 7 | Kinetics of CAP degradation at different initial concentration (a) Kinetic curves (b) the variation of reaction rate constants.

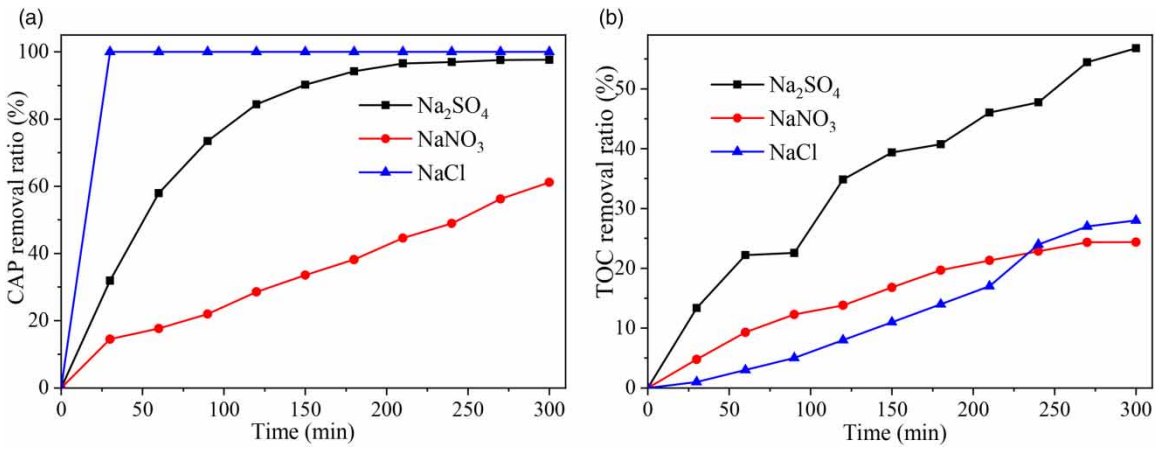

Figure 8 | (a) CAP removal ratio and (b) TOC removal ratio in different electrolytes of Na_2SO_4, $NaNO_3$ and NaCl.

to $\cdot SO_4^-$ (Equations (6)–(8)), which has a similar oxidation ability to ·OH (Davis *et al.* 2014; Hu *et al.* 2018; Zhang *et al.* 2020a, 2020b). Accordingly, the removal ratio of CAP and TOC were high in sodium sulfate medium:

$$SO_4^{2-} \rightarrow \cdot SO_4^- + e^- \quad (6)$$

$$HSO_4^- + \cdot OH \rightarrow \cdot SO_4^- + H_2O \quad (7)$$

$$H_2SO_4 + \cdot OH \rightarrow \cdot SO_4^- + H_3O^+ \quad (8)$$

$$\cdot OH + Cl^- \rightarrow \cdot ClOH^- \quad (9)$$

Effect of electrolyte concentration

The electrolyte concentration has a significant effect on a conductance of the solution. CAP removal depends on a conductance of the solution too. The variation of CAP removal ratio with time is shown in Figure 9. The inner figure shows the variation of conductance with Na_2SO_4 concentration. Conductance of the solution was increasing with concentration of Na_2SO_4 when Na_2SO_4 concentration varied from 1.25 g L^{-1} to 25 g L^{-1}. The CAP removal ratio was 98.0% at Na_2SO_4 concentration of 6.25 g L^{-1}. When the concentration of electrolyte in the solution was excessively high, the generation of free radicals was inhibited. Excessive ions affected the diffusion of free radicals to aqueous solution, which affected the degradation of organic pollutants in water.

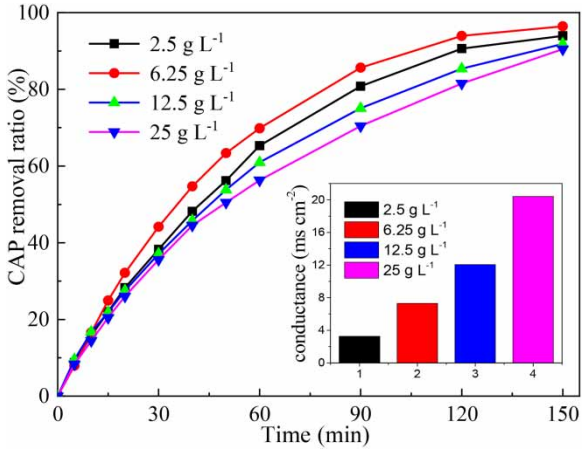

Figure 9 | The variation of CAP removal ratio with time.

Effect of ethanol and tertiary butanol

Figure 10 shows the effects of ethanol and tertiary butanol (free radical quencher) on the removal of CAP (Figure 9(a)) and TOC (Figure 9(b)). Ethanol was used to quench ·OH and $\cdot SO_4^-$, and tertiary butanol was used to quench ·OH (Tan *et al.* 2018). The removal ratio of CAP with ethanol (42.0%) was much lower than that without quencher(100.0%). The removal ratio of CAP with tertiary butanol was slightly lower than that without a quencher. This indicated that in this electrochemical system, $\cdot SO_4^-$ and direct oxidation contributed much to the degradation of CAP. In the absence of quencher, the mineralization of CAP was highest. Therefore, the degradation of CAP on the Ti-based SnO_2–Sb–Ni electrode in a single chamber resulted from the synergistic effect of direct oxidation and indirect oxidation (·OH and $\cdot SO_4^-$).

Comparison of oxidation and reduction of CAP

The treatment of CAP by electrochemical processes was conducted in a divided chamber. CAP was oxidized in an anode chamber and reduced in a cathode chamber. The removal ratio of CAP, the removal ratio of TOC and antibacterial activity by oxidation and reduction are compared in Table 1. Through the comparison, CAP was completely removed by reduction in the cathode chamber. Nevertheless, the removal ratio of TOC in the cathode chamber was low. The cathodic reduction can only remove halogen and nitro group from CAP and reduce toxicity. CAP cannot be completely mineralized by cathodic reduction. This was consistent with the results reported in the literature. For the CAP reduction, four main products, nitroso product (NO), aromatic amine product ($AMCl_2$) and dechlorinated $AMCl_2$ products (AMCl and AM) were detected using

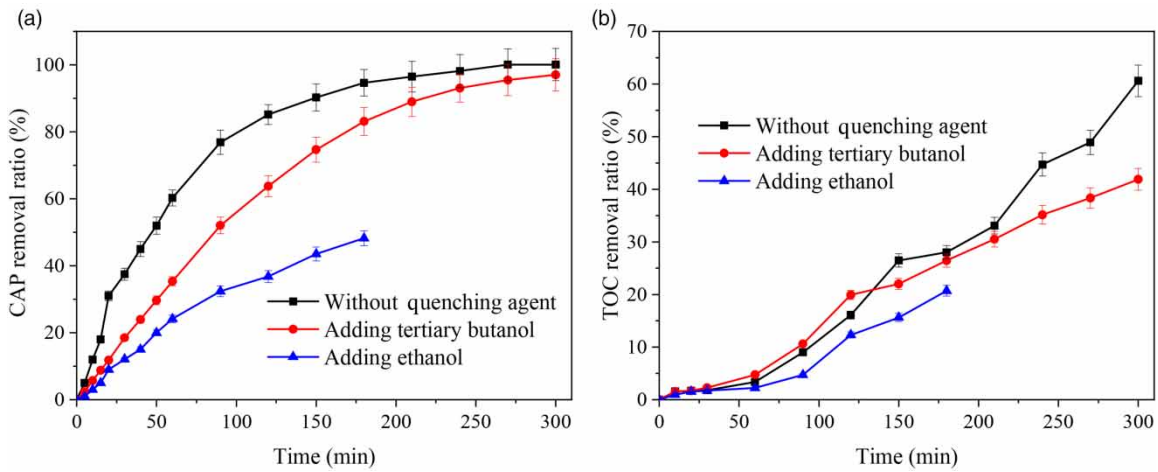

Figure 10 | (a) CAP removal ratio and (b) TOC removal ratio with different quenchers.

Table 1 | The comparison of the removal ratio of CAP, the removal ratio of TOC and antibacterial activity by oxidation and reduction

Parameter	Raw water	Single chamber	Divided chamber (anode chamber)	Divided chamber (cathode chamber)	Reduction of CAP (Liang *et al.* 2012)
Removal ratio of CAP(%)	0	100%	92.58%	100%	99.86
Removal ratio of TOC(%)	0	56.68%	47.91%	4.62%	0
Diameter of bacteriostatic ring (mm)	25	0	0	19	–

high performance liquid chromatography. The intermediate NO slightly accumulated initially and then quickly reduced to amine products under the cathode potentials between −0.75 and −1.25 V. $AMCl_2$ could be accumulated when the cathode potential was higher than −0.75 V. When the cathode potential was lower than −0.41 V, $AMCl_2$ could be fractional reduced to the dechlorinated product AMCl when the cathode potential was −0.45 V. AMCl could be further dechlorinated only when the cathode potential was lower than −0.95 V (Kong *et al.* 2015). The mineralization of CAP was improved by anodic oxidation in the anode chamber. In a single chamber, the effects of CAP removal and mineralization are enhanced, which were contributed to the synergism of oxidation and reduction. After 300 min reaction, CAP had no antimicrobial activity in a single chamber and anode chamber. CAP maintained certain antimicrobial activity in the cathode chamber. This may be due to the removal of functional groups with antimicrobial activity by anodic oxidation. Therefore, anodic oxidation was more effective for the removal of CAP. CAP was almost eliminated by cathodic reduction and the mineralization ratio was quite low. However, it may be easier to achieve complete mineralization by further treatment after cathodic reduction (Liang *et al.* 2012).

CONCLUSIONS

This study reported the preparation of a Ti-based SnO_2–Sb–Ni electrode and its application for the degradation of CAP. Due to the doping of transition metal nickel, the surface of the Ti-based SnO_2–Sb–Ni electrode was more compact and uniform than the Ti-based SnO_2–Sb electrode. Compared to the Ti-based SnO_2–Sb electrode, the addition of nickel improved the oxidation performance of the Ti-based SnO_2–Sb–Ni electrode and the mineralization of CAP. For 100 mg L^{-1} CAP, 100% CAP removal ratio and 60% TOC removal ratio could be achieved for 300 min treatment at the current density of 20 mA cm^{-2} and in neutral electrolyte (6.25 g L^{-1} Na_2SO_4). The electro-oxidation of CAP on the Ti-based SnO_2–Sb–Ni electrode displayed a pseudo-first-order kinetic model. Free radical quenching experiments have shown that the oxidation of CAP on the Ti-based SnO_2–Sb–Ni electrode resulted from the synergistic effect of direct oxidation and indirect oxidation (·OH and $\cdot SO_4^-$). Direct oxidation and $\cdot SO_4^-$ contributed much to the degradation of CAP. In the process of cathodic reduction, the removal ratio of CAP was high, while the removal ratio of TOC was low. Anodic oxidation was more effective for the removal of CAP.

ACKNOWLEDGEMENTS

The project was supported by the 'LiaoNing Revitalization Talents Program (XLYC1908034)', 'Liaoning BaiQianWan Talents Program' and 'Liaoning Technology Innovation Center of Water Treatment and Resource'.

DATA AVAILABILITY STATEMENT

All relevant data are included in the paper or its Supplementary Information.

REFERENCES

Amildon Ricardo, I., Paiva, V. A. B., Paniagua, C. E. S. & Trovó, A. G. 2018 Chloramphenicol photo-Fenton degradation and toxicity changes in both surface water and a tertiary effluent from a municipal wastewater treatment plant at near-neutral conditions. *Chemical Engineering Journal* **347**, 763–770.

Asim, S., Zhu, Y., Batool, A., Hailili, R., Luo, J., Wang, Y. & Wang, C. 2017 Electrochemical treatment of 2,4-dichlorophenol using a nanostructured 3D-porous Ti/Sb-SnO_2-Gr anode: reaction kinetics, mechanism, and continuous operation. *Chemosphere* **185**, 11–19.

Berenguer, R., Sieben, J. M., Quijada, C. & Morallon, E. 2014 Pt- and Ru-doped SnO_2–Sb anodes with high stability in alkaline medium. *ACS Applied Materials & Interfaces* **6** (24), 22778–22789.

Chang, X., van der Zalm, J., Thind, S. S. & Chen, A. 2020 Electrochemical oxidation of lignin at electrochemically reduced TiO_2 nanotubes. *Journal of Electroanalytical Chemistry* **863**, 114049.

Comninellis, C. & Pulgarin, C. 1993 Electrochemical oxidation of phenol for wastewater treatment using SnO_2 anodes. *Journal of Applied Electrochemistry* **23**, 108–112.

Davis, J., Baygents, J. C. & Farrell, J. 2014 Understanding persulfate production at boron doped diamond film anodes. *Electrochimica Acta* **150**, 68–74.

Fernández-Aguirre, M. G., Berenguer, R., Beaumont, S., Nuez, M., La Rosa-Toro, A., Peralta-Hernández, J. M. & Morallón, E. 2020 The generation of hydroxyl radicals and electro-oxidation of diclofenac on Pt-doped SnO_2–Sb electrodes. *Electrochimica Acta* **354**, 136686.

Hamed, S. & Amini, M. K. 2011 Effect of elemental composition on the structure, electrochemical properties, and ozone production activity of Ti/SnO_2–Sb–Ni electrodes prepared by thermal pyrolysis method. *International Journal of Electrochemistry* **2011**, 1–13.

He, Y., Lin, H., Guo, Z., Zhang, W., Li, H. & Huang, W. 2019 Recent developments and advances in boron-doped diamond electrodes for electrochemical oxidation of organic pollutants. *Separation and Purification Technology* **212**, 802–821.

Hems, R., Gauthier-Signore, C., Bejan, D. & Bunce, N. J. 2016 Kinetic models for the oxidation of organic substrates at boron-doped diamond anodes. *Chemical Engineering Journal* **300**, 404–413.

Hu, L., Zhang, G., Wang, Q., Sun, Y., Liu, M. & Wang, P. 2018 Facile synthesis of novel Co_3O_4–Bi_2O_3 catalysts and their catalytic activity on bisphenol A by peroxymonosulfate activation. *Chemical Engineering Journal* **326**, 1095–1104.

Jan, O. B., Thomas, O., Karl, W., Simon, J. & Marco, R. 2018 Combining ultrafiltration and non-thermal plasma for low energy degradation of pharmaceuticals from conventionally treated wastewater. *Journal of Environmental Chemical Engineering* **6** (6), 7377–7385.

Kaur, R., Kushwaha, J. P. & Singh, N. 2018 Electro-oxidation of ofloxacin antibiotic by dimensionally stable Ti/RuO_2 anode: evaluation and mechanistic approach. *Chemosphere* **193**, 685–694.

Kaur, R., Kushwaha, J. P. & Singh, N. 2019 Amoxicillin electro-catalytic oxidation using Ti/RuO_2 anode: mechanism, oxidation products and degradation pathway. *Electrochimica Acta* **296**, 856–866.

Kimosop, S. J., Getenga, Z. M., Orata, F., Okello, V. A. & Cheruiyot, J. K. 2016 Residue levels and discharge loads of antibiotics in wastewater treatment plants (WWTPs), hospital lagoons, and rivers within Lake Victoria basin, Kenya. *Environmental Monitoring and Assessment* **188** (9), 532.

Kong, D., Liang, B., Yun, H., Cheng, H., Ma, J., Cui, M., Wang, A. & Ren, N. 2015 Cathodic degradation of antibiotics: characterization and pathway analysis. *Water Research* **72**, 281–292.

Laquaz, M., Dagot, C., Wiest, L., Bazin, C., Gaschet, M. & Perrodin, Y. 2020 Ecotoxicity and antibiotic resistance of wastewater during transport in an urban sewage network. *Environmental Science and Pollution Research (international)* **27** (16), 19991–19999.

Li, J., Cheng, W., Xu, L., Jiao, Y., Baig, S. A. & Chen, H. 2016 Occurrence and removal of antibiotics and the corresponding resistance genes in wastewater treatment plants: effluents' influence to downstream water environment. *Environmental Science and Pollution Research (international)* **23** (7), 6826–6835.

Liang, B., Jiang, J., Zhang, J., Zhao, Y. & Li, S. 2012 Horizontal transfer of dehalogenase genes involved in the catalysis of chlorinated compounds: evidence and ecological role. *Critical Reviews of Microbiology* **38** (2), 95–110.

Liang, J. Y., Geng, C., Li, D., Cui, L. & Wang, X. 2015 Preparation and degradation phenol characterization of Ti/SnO_2–Sb-Mo electrode doped with different contents of molybdenum. *Journal of Materials Science and Technology* **31** (5), 473–478.

Liang, J. Y., Geng, C., Li, D., Yuan, F. Y., Cui, L. & Wang, X. 2016 Research progress on the modification and application of antimony-doped tin dioxide electrodes. *Rare Metal Materials and Engineering* **45** (3), 810–814.

Marcelino, R. B., Queiroz, M. T., Amorim, C. C., Leao, M. M. & Brites-Nobrega, F. F. 2015 Solar energy for wastewater treatment: review of international technologies and their applicability in Brazil. *Environmental Science and Pollution Research (international)* **22** (2), 762–773.

Montilla, F., Morallón, E., De Battisti, A. & Vázquez, J. L. 2004 Preparation and characterization of antimony-doped tin dioxide electrodes. Part 1. Electrochemical characterization. *Journal of Physical Chemistry B* **108**, 5036–5043.

Moreira, F. C., Boaventura, R. A. R., Brillas, E. & Vilar, V. J. P. 2017 Electrochemical advanced oxidation processes: a review on their application to synthetic and real wastewaters. *Applied Catalysis B: Environmental* **202**, 217–261.

Novak Jovanović, I., Miličević, A., Jadreško, D. & Hranjec, M. 2020 Electrochemical oxidation of synthetic amino-substituted benzamides with potential antioxidant activity. *Journal of Electroanalytical Chemistry* **870**, 114244.

Panizza, M. & Cerisola, G. 2009 Direct and mediated anodic oxidation of organic pollutants. *Chemical Reviews* **109**, 6541–6569.

Qiang, L., Lichao, A., Qin, Z., Wenwen, X. & Zhiliang, W. 2010 Treatment of nitrobenzene wastewater by electrocatalytic oxidation with Sn-Sb/Ti electrode. *Environmental Protection of Chemical Industry* **30** (2), 100–103.

Radko, L., Sniegocki, T., Sell, B. & Posyniak, A. 2019 Metabolomic profile of primary turkey and rat hepatocytes and two cell lines after chloramphenicol exposure. *Animals (Basel)* **10** (1), 1–15.

Rubí-Juárez, H., Cotillas, S., Sáez, C., Cañizares, P., Barrera-Díaz, C. & Rodrigo, M. A. 2016 Use of conductive diamond photo-electrochemical oxidation for the removal of pesticide glyphosate. *Separation and Purification Technology* **167**, 127–135.

Salazar, C., Contreras, N., Mansilla, H. D., Yanez, J. & Salazar, R. 2016 Electrochemical degradation of the antihypertensive losartan in aqueous medium by electro-oxidation with boron-doped diamond electrode. *Journal of Hazardous Materials* **319**, 84–92.

Sharpe, R., Munarriz, J., Lim, T., Jiao, Y., Niemantsverdriet, J. W., Polo, V. & Gracia, J. 2018 Orbital physics of perovskites for the oxygen evolution reaction. *Topics in Catalysis* **61** (3–4), 267–275.

Stucki, S., Kotz, R., Carcer, B. & Suter, W. 1991 Electrochemical waste water treatment using high overvoltage anodes. Part II: Anode performance and applications. *Journal of Applied Electrochemistry* **21**, 99–104.

Sun, Y. J., Chen, A. W., Sun, W. Q., Zhou, J., Shah, K. J., Zheng, H. L. & Shen, H. 2019 Degradation of chloramphenicol by Ti-Ag/gamma-Al_2O_3 particle electrode using three-dimensional reactor. *Desalination and Water Treatment* **163**, 96–108.

Tan, C., Dong, Y., Shi, L., Chen, Q., Yang, S., Liu, X., Ling, J., He, X. & Fu, D. 2018 Degradation of orange II in ferrous activated peroxymonosulfate system: efficiency, situ EPR spin trapping and degradation pathway study. *Journal of the Taiwan Institute of Chemical Engineers* **83**, 74–81.

Wu, M., Tang, Y., Liu, Q., Tan, Z., Wang, M., Xu, B., Xia, S., Mao, S. & Gao, N. 2020 Highly efficient chloramphenicol degradation by UV and UV/H_2O_2 processes based on LED light source. *Water Environment Research* **92** (12), 2049–2059.

Yerabham, P., Akiba, M., Guruge, K. S., Balakrishna, K., Vandana, K. E. & Kumar, V. 2020 Occurrence of antimicrobial-resistant *Escherischia coli* in sewage treatment plants of south India. *Journal of Water Sanitation and Hygiene for Development* **10** (1), 48–55.

Yu, J., Hou, X., Hu, X., Yuan, H., Wang, J. & Chen, C. 2019 Efficient degradation of chloramphenicol by zero-valent iron microspheres and new insights in mechanisms. *Applied Catalysis B: Environmental* **256**, 117876.

Zhang, F., Sun, Z. & Cui, J. 2020a Research on the mechanism and reaction conditions of electrochemical preparation of persulfate in a split-cell reactor using BDD anode. *RSC Advances* **10** (56), 33928–33936.

Zhang, Y. L., Kokswee, G., Zhao, L., Sui, X. L., Gong, X. F., Cai, J. J., Zhou, Q. Y., Zhang, H. D., Li, L., Kong, F. R., Gu, D. M. & Wang, Z. B. 2020b Advanced non-noble materials in bifunctional catalysts for ORR and OER toward aqueous metal-air batteries. *Nanoscale* **12** (42), 21534–21559.

Zhou, Y., Wang, T., Zhi, D., Guo, B., Zhou, Y., Nie, J., Huang, A., Yang, Y., Huang, H. & Luo, L. 2019 Applications of nanoscale zero-valent iron and its composites to the removal of antibiotics: a review. *Journal of Materials Science* **54** (19), 12171–12188.

First received 19 March 2021; accepted in revised form 1 June 2021. Available online 15 June 2021